

## Impact of $T_e/T_i$ on confinement properties with emphasis on profile shapes

$T_e/T_i$ の閉じ込め性能に対する寄与と分布形状効果に関する研究

Emi Narita<sup>1</sup>, Tomonori Takizuka<sup>1,2</sup>, Nobuhiko Hayashi<sup>2</sup>, Takaaki Fujita<sup>2</sup>, Shunsuke Ide<sup>2</sup>, Mitsuru Honda<sup>2</sup>, Yasuyuki Tanaka<sup>1</sup>, Akihiko Isayama<sup>2</sup>, Kiyoshi Itami<sup>2</sup> and Takeshi Fukuda<sup>1</sup>  
 成田絵美<sup>1</sup>, 滝塚知典<sup>1,2</sup>, 林伸彦<sup>2</sup>, 藤田隆明<sup>2</sup>, 井手俊介<sup>2</sup>, 本多充<sup>2</sup>, 田中靖之<sup>1</sup>, 諫山明彦<sup>2</sup>,  
 伊丹 潔<sup>2</sup>, 福田武司<sup>1</sup>

<sup>1</sup>Osaka University

2-1 Yamadaoka, Suita, Osaka 56-0871, Japan

大阪大学大学院 〒565-0871 大阪府吹田市山田丘2-1

<sup>2</sup>Japan Atomic Energy Agency

801-1 Mukoyama, Naka, Ibaraki 311-0193, Japan

日本原子力研究開発機構 〒311-0193 茨城県那珂市向山801-1

In order to know the impact of the temperature ratio  $T_e/T_i$  on confinement properties, the updated DB3v10 database has been analyzed. It is suggested that the increasing in  $T_e/T_i$  deteriorates the confinement in peaked density regime. This result has been checked against the simulation for JT-60SA using the transport code TOPICS with the GLF23 transport model module and the GS2 code. As a consequence, these results qualitatively agree with each other.

### 1. Introduction

The IPB98(y,2) scaling law<sup>[1]</sup>, which has been widely used for predicting the performance of future devices, was elaborated from largely consists of dominantly ion-heated discharges. In a future burning machine, like ITER, on the contrary, it is expected that  $T_e/T_i$  is larger than unity due to the strong alpha heating. In order to understand the impact of  $T_e/T_i$  on confinement properties, we have studied the updated DB3v10 database<sup>[1,2]</sup>, with emphasis on the  $T_e/T_i$  effect. The impact has been also investigated by using the transport code TOPICS<sup>[3]</sup> with GLF23 transport model module and the code GS2<sup>[4]</sup>.

### 2. Scaling analyses with emphasis on the $T_e/T_i$

The 317 data from JET, 67 from AUG and 68 from C-Mod have been extracted from the database. For these data, the central temperature ratio  $T_{e0}/T_{i0}$  is limited in the range  $0.5 < T_{e0}/T_{i0} < 1.5$ , the peaking factor, which is defined as the ratio of central density and line averaged density, is limited in the range  $1.0 < n_{e0}/n_e < 1.6$ , and the line averaged density is lower than 60% of  $n_{GW}$ . As a consequence of regression analyses, we have obtained following scaling expressions in two peaking factor regimes;

$$\tau_{sc1} = 0.0777 I_p^{0.91} B_t^{0.11} n_e^{0.28} P_L^{-0.59} R^{1.73} M^{0.27} \varepsilon^{0.54} \kappa^{0.41}$$

;  $1.0 < n_{e0}/n_e < 1.1$  (flat density case), (1)

$$\tau_{sc2} = 0.0594 I_p^{0.90} B_t^{0.08} n_e^{0.34} P_L^{-0.63} R^{1.78} M^{0.16} \varepsilon^{0.41} \kappa^{0.72}$$

;  $1.1 < n_{e0}/n_e < 1.6$  (peaked density case). (2)

The notations comply with conventional definitions. Histograms of  $\tau_{th}/\tau_{sc1}$  and  $\tau_{th}/\tau_{sc2}$  for  $T_{e0}/T_{i0} < 1$  and

$T_{e0}/T_{i0} > 1$  are shown in Fig.1. Fig.1(a) and (c) describe that the peaked density profile improves the confinement for discharges with  $T_{e0}/T_{i0} < 1$ , whereas, it works adversely in the  $T_{e0}/T_{i0} > 1$  case.

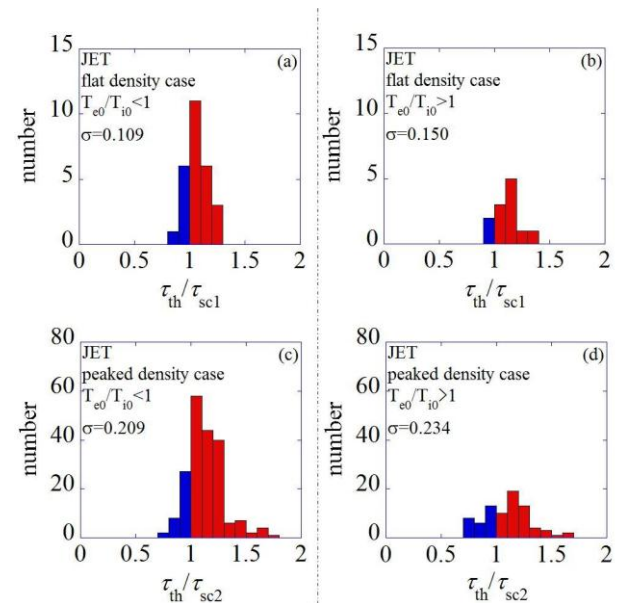


Fig.1. Histograms  $\tau_{th}/\tau_{sc1}$  and  $\tau_{th}/\tau_{sc2}$ . (a) and (b) flat density case, (c) and (d) peaked density case.  $T_{e0}/T_{i0} < 1$  data are shown in (a) and (c).  $T_{e0}/T_{i0} > 1$  data are shown in (b) and (d).

For the latter, we have further developed a scaling expression including  $T_e/T_i$  for peaked density case. We incorporated 3 nondimensional variables<sup>[5]</sup>, namely  $B_t R^{1.25}$ ,  $n_e/n_{GW}^*$ , and  $q$  in addition to  $T_e/T_i$ .

Here,  $n_e/n_{GW}^*$  is dimensionless normalized density. The dependences on  $n_e/n_{GW}^*$  and  $q$  were weak, and the following new expression was obtained; which reduce the standard deviation remarkably,

$$\tau_{sc3} = \tau_{sc2} \{ 1 - 0.157(T_{e0}/T_{i0} - 1)(B_t R^{1.25})^{0.59} \}. \quad (3)$$

Here, we find that the confinement time decreases with increasing  $T_{e0}/T_{i0}$  [6]. The correction term  $f = 0.157(T_{e0}/T_{i0} - 1)(B_t R^{1.25})^{0.59}$  in (3) was plotted against  $n_{e0}/n_e$  for large and small values of  $T_{e0}/T_{i0}$ . It is deduced that peaked density profiles contribute to an improvement for low value of  $T_{e0}/T_{i0}$  region and deteriorate for high value of the ratio region.

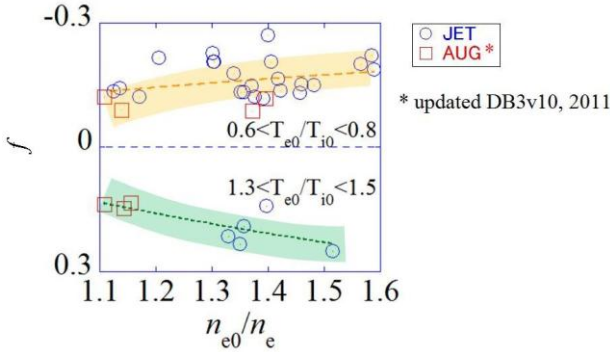


Fig. 2. Dependence of the correction term  $f$  in (3) on peaking factor  $n_{e0}/n_e$  for large and small values of temperature ratio.

### 3. Simulations with GLF23 and GS2

The impact of  $T_e/T_i$  on confinement with emphasis on the density profile is demonstrated by simulations using the transport code TOPICS with the GLF23 transport model module and using the code GS2. GLF module suggests that the transport is enhanced for large  $T_e/T_i$  regime [7], and the code GS2 is effective to investigate the low-frequency turbulence in magnetized plasmas.

We investigated the effect of  $T_{e0}/T_{i0}$  in four types of density profiles using TOPICS with GLF23. The value of  $T_{e0}/T_{i0}$  is varied by the ratio between heating power for electrons and that for ions. The effects of  $\alpha$  stabilization and ExB shear stabilization are included in these simulations. Fig. 3(a) shows the dependence of  $H_H$ -factor on  $T_{e0}/T_{i0}$  for different density profiles. Here,  $H_H$ -factor is defined as  $H_H = \tau_{th} / \tau_{IPB98(y,2)}$ . The dependence of derivative value of  $H_H$ -factor with respect to  $T_{e0}/T_{i0}$  as a function of peaking factor is demonstrated in Fig. 3(b). The effect of  $T_{e0}/T_{i0}$  becomes more profound with the increasing of peaking factor. This agrees with the results from scaling analyses.

The influences of  $T_{e0}/T_{i0}$  and  $n_{e0}/n_e$  have also been investigated with the GS2 code. Fig. 4

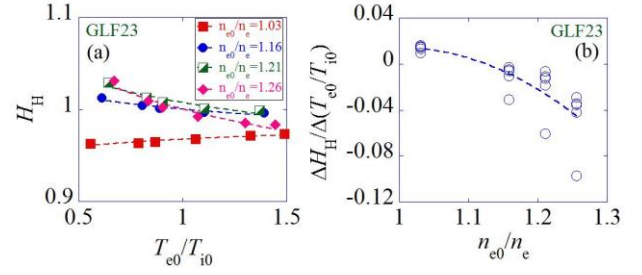


Fig. 3. (a) Dependence of  $H_H$ -factor on  $T_{e0}/T_{i0}$  for different density profiles. (b) Derivatives of  $H_H$ -factor for  $T_{e0}/T_{i0}$  against the density peaking factor. Here,  $I_p \approx 2.3$  MA,  $B_t \approx 1.7$  T,  $q_{95} \approx 4.7$ ,  $\kappa \approx 1.9$  and  $\delta \approx 0.49$ .

indicates increased linear growth rate and larger amplitude of potential fluctuation at larger  $T_{e0}/T_{i0}$  in higher normalized wave number. Fig. 4(a) also shows that the effect of  $T_{e0}/T_{i0}$  on linear growth rate is slightly higher in the peaked density profile at larger  $T_{e0}/T_{i0}$ , and Fig. 4(b) shows that the effect on energy flux is stronger in the peaked density profile. These impacts of  $T_{e0}/T_{i0}$  and  $n_{e0}/n_e$  are consistent with results of the database analyses.

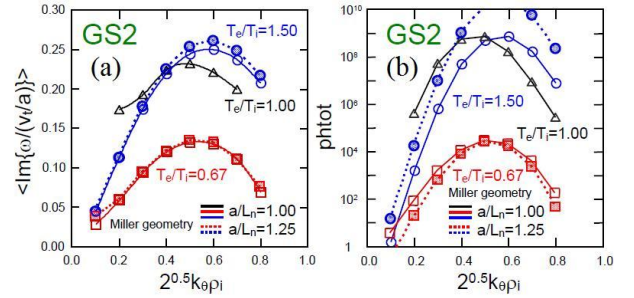


Fig. 4. Dependences of (a) growth rate and (b) amplitude of potential fluctuation on normalized wave number. Here,  $q_{95} \approx 3.03$ ,  $\kappa \approx 1.66$  and  $\delta \approx 0.429$ .

### References

- [1] Progress in the ITER Physics Basis, Chapter 2: Plasma confinement and transport, Nucl. Fusion **47** S18 (2007)
- [2] The international global H-mode confinement database <http://efdsql.ipp.mpg.de/hmodepublic/>
- [3] N. Hayashi, et al., J. Plasma Fusion Res. **80**, 605-613 (2004)
- [4] Sources downloaded from <http://www.gs2.sourceforge.net/>, M. Kotschenreuther, G. Rewoldt, and W.M. Tang, Comp. Phys. Comm. **88**, 128 (1995)
- [5] T Takizuka JAERI-Research 95-075 (1995)
- [6] E Narita 2011 38<sup>th</sup> EPS Conf. on Plasma Physics (Strasbourg) P2.121 <http://ocs.ciemat.es/EPS2011PAP/pdf/P2.121.pdf>
- [7] R. E. Waltz, et al., Phys. Plasmas **4**, 2482 (1997)